Electronic Supplementary Material (ESI) for Energy & Environmental Science.

Reconsidering Figures of Merit for Performance and Stability of Perovskite Photovoltaics

Mark V. Khenkin,[1] Anoop K.M.,[1] Iris Visoly-Fisher,[1,2] Yulia Galagan,[3] Francesco Di Giacomo,[3] Bhushan Ramesh Patil[4], Golnaz Sherafatipour[4], Vida Turkovic[4], Horst-Günter Rubahn,[4] Morten Madsen,[4] Tamara Merckx, [5] Griet Uytterhoeven, [5] João P. A. Bastos,[5,6] Tom Aernouts,[5] Francesca Brunetti,[7] Monica Lira-Cantu[8] and Eugene A. Katz[1,2,*]

[1]Dept. of Solar Energy and Environmental Physics, Swiss Inst. for Dryland Environmental and Energy Research, J. Blaustein Institutes for Desert Research, Ben-Gurion University of the Negev, Midreshet Ben-Gurion 8499000, Israel

[2]Ilse Katz Institute for Nanoscale Science and Technology, Ben-Gurion University of the Negev, Beersheva 8410501, Israel

[3]Holst Centre – Solliance, High Tech Campus 21, 5656 AE, Eindhoven, the Netherlands

[4]SDU NanoSYD, Mads Clausen Institute, University of Southern Denmark, Alsion 2, DK-6400 Sønderborg, Denmark

[5]IMEC – a partner in Solliance, Kapeldreef 75, 3000 Leuven, Belgium

[6]Department Electrical Engineering, KU Leuven, 3001 Leuven, Belgium

[7] CHOSE (Centre for Hybrid and Organic Solar Energy), Department of Electronic Engineering, University of Rome Tor Vergata, via del Politecnico 1, 00133 Rome, Italy

[8]Catalan Institute of Nanoscience and Nanotechnology (ICN2), CSIC and The Barcelona Institute of Science and Technology, Campus UAB, Bellaterra E-08193, Barcelona, Spain

e-mail: keugene@bgu.ac.il

Supporting Information

Degradation of devices of type 1 under continuous illumination by simulated sunlight indoors.

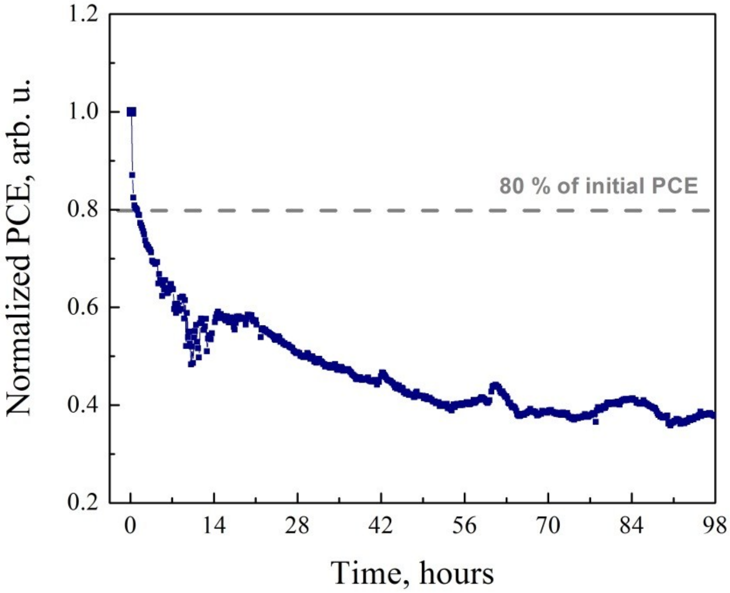

Figure S1. Normalized *PCE* evolution of the glass/ITO/$\mathrm{SnO_2}$/$\mathrm{Cs_{0.05}((CH_3NH_3)_{0.15}(CH(NH_2)_2)_{0.85})_{0.95}PbI_{2.55}Br_{0.45}}$/Spiro-OMeTAD /Au cells (type I) during continuous illumination by simulated sunlight indoors**.**

E_{80} calculation

As described in the manuscript, E_{80} values were calculated using either Eq. (1) or Eq. (3) with P_{in} set to 1 sun for simplicity. This value is proportional to the area below the curve of the *PCE* versus time of sunlight exposure shown in Figure S2. The area below the curve that accounts for *PCE* diurnal dynamics is substantially smaller than the area below the curve that corresponds to maximal during-the-day *PCE* values. For example, for a cell of type I (Figure S2a), the overestimation of E_{80} is as high as ~20% for first four days of exposure (T_{80}^{max} = 4 d). Note that the faster the daily changes for type I cells are, and the slower the daily changes for type II cells are, the greater is the difference between these areas.

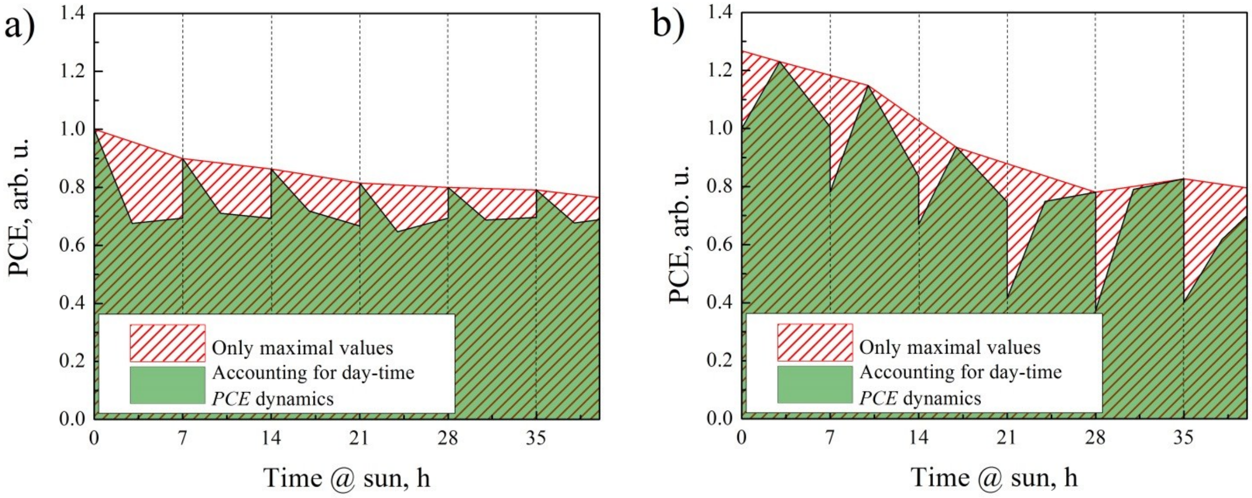

Figure S2. Area under the *PCE* versus time accounting only for maximal during-the-day values (red stripes) and for all measured during the day values (green) for (a) type I devices and (b) type II devices.

Device preparation and initial performance characterization.

Glass/ITO/SnO_2 /$Cs_{0.05}(CH_3NH_3)_{0.15}(CH(NH_2)_2)_{0.85})_{0.95}Pb(I_{2.55}Br_{0.45})$/Spiro-OMeTAD/Au cells (type I)

Glass substrates of 3 cm × 3 cm with patterned ITO electrodes were purchased from Naranjo. The substrates were cleaned by sequential sonication in a detergent solution, deionized water, and isopropanol. The substrates were then treated with UV-O3 for 30 min.

A tin oxide (SnO_2) nanoparticle solution (15 wt.%), purchased from Alfa Aesar, was diluted by water in a volume ratio of 1:5. Spin-coating of the SnO_2 solution on glass/ITO substrates was performed with a spin speed of 2800 rpm for 50 s and annealed for 30 min at 150 °C. The SnO_2 layer's resulting thickness was 30-40 nm. After preparing the SnO_2, samples were transferred to a N_2-filled glove-box for the perovskite deposition.

Lead iodide (PbI_2) (TCI) and formadiniun iodide (FAI) (Dyesol) with a molar ratio of 1.3:1.17 were dissolved in an N,N-dimethylformamide (DMF): dimethyl sulfoxide (DMSO) solution (volume ratio of 9:1). Lead bromide ($PbBr_2$) (TCI) and methylammonium bromide (MABr) (Dyesol) with a molar ratio of 1.3:1.3 were dissolved in a DMF:DMSO solution (volume ratio of 9:1). Cesium iodide (CsI) (Sigma Aldrich) was dissolved in pure DMSO, forming a 1.5 M solution. The three solutions were stirred for at least 60 min before use. Then the three solutions were mixed together, in order to fabricate the mixed-cation, mixed-halide perovskite phase $Cs_{0.05}(MA_{0.15}FA_{0.85})_{0.95}PbI_{2.55}Br_{0.45}$. The resulting solution was spin-coated at 5000 rpm for 50 s onto a SnO_2-coated substrate. During spin-coating, 210 μL of an antisolvent (chlorobenzene) was dropped onto the substrate at the 40th s of spin-coating. Samples were transferred to a hotplate for annealing at 100 °C for 30 min, resulting in a perovskite layer of 500 nm.

The Spiro-OMeTAD solution (80 mg of Spiro-O-MeTAD (Lumtec), 28 μl of 4-tert-butylpyridine, 17.5 μl of a 520 mg ml^{-1} $LiN(CF_3SO_2)_2N$ solution in acetonitrile and 20 μl of a 500 mg ml^{-1} FK209 cobalt salt solution in acetonitrile were added to 1 ml of chlorobenzene) was spin-casted in air at 2000 rpm for 60 s onto the perovskite film, resulting in the formation of a 200-nm-thick hole transporting layer. Complete Spiro-OMeTAD oxygen doping was attained by exposing the substrates to air under controlled humidity (RH = 48%) for an additional 30 min. Subsequently, the substrates were transferred to the thermal evaporator under a pressure of 1.0×10^{-6} mbar, where a 100-nm Au back electrode was deposited on top of the Spiro-OMeTAD film. During the Au evaporation, a shadow mask was placed on each substrate, where the overlap between the ITO and Au electrodes determined the active device area of 0.16 cm^2. Encapsulation of the devices was performed by lamination of a barrier film (R2R manufactured at the Holst Centre)[1] with a pressure-sensitive adhesive. The edge of the substrate was cleaned from the materials to ensure proper adhesion of the barrier film to the glass substrate at the edge, and thereby prevent de-lamination and slow down the side ingress of water and oxygen.

Initial J-V measurements were carried out under simulated AM 1.5 G sunlight conditions, using MiniSunSim simulator (calibrated with c-Si cells) and a Keithley 2400 source meter unit. Devices were measured in both forward and reverse directions with a scan rate of 300 mV/s and then were tracked at the maximum power point (MPPT) for >120 s in order to get the stabilized value. A shadow mask of 0.09 cm2 was used to better define the active area. The average MPPT efficiency of the devices was 16%. The typical J-V curve is shown in Figure S3a, and the average performance of 32 identical devices is shown in Figure S3b.

The EQE spectra of the cells were measured using a PV spectral response measurement system ("TECHNOEXAN" Ltd., Ioffe Physical-Technical Institute, Russia). The spectra were recorded as a function of wavelength by focusing light from a halogen lamp by means of a parabolic mirror on the input slot of a grating monochromator with automatic grating switching. In front of the slot, a chopper rotated by a synchronous motor was placed in order to use lock-in amplified detection of the signals. The overall spectral range is covered using two gratings: P1 (for the range 320– 540 nm) and P2 (400–1200 nm range). The grating change between P1 and P2 occurred at 500 nm. The modulated light passes through the monochromator to an output slot equipped with a diaphragm. The chopper's frequency was set to 75 Hz. The typical EQE spectrum is shown in Figure S4.

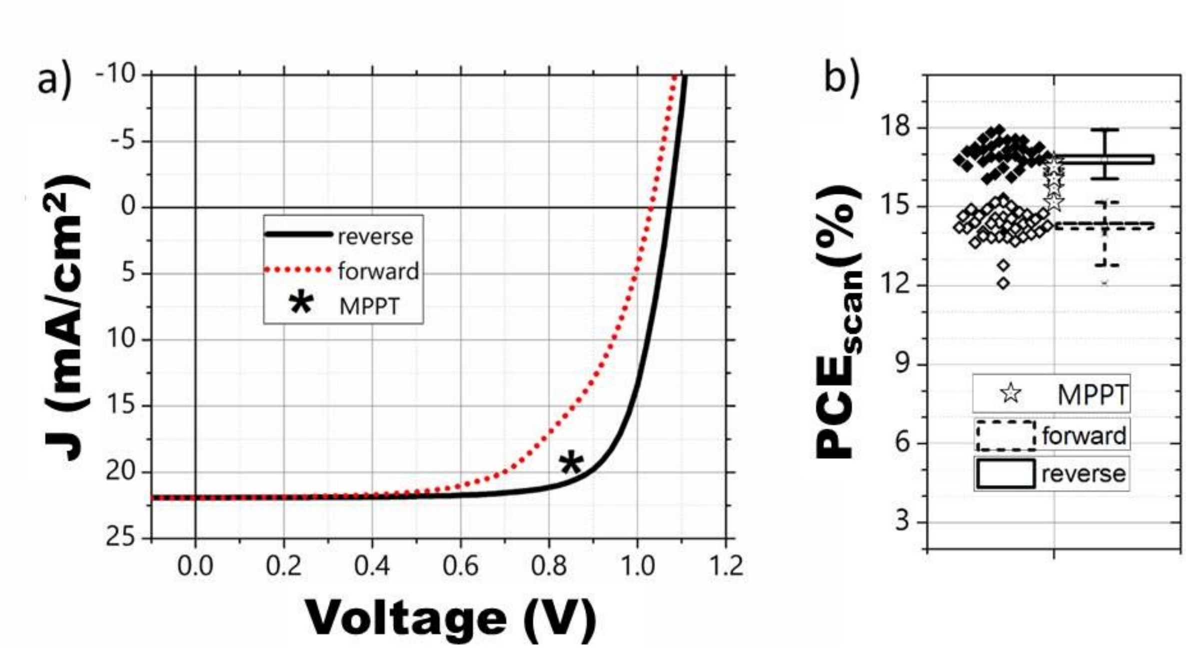

Figure S3. (a) Typical *J-V* characteristic of the type I devices, and (b) average performance of the manufactured devices.

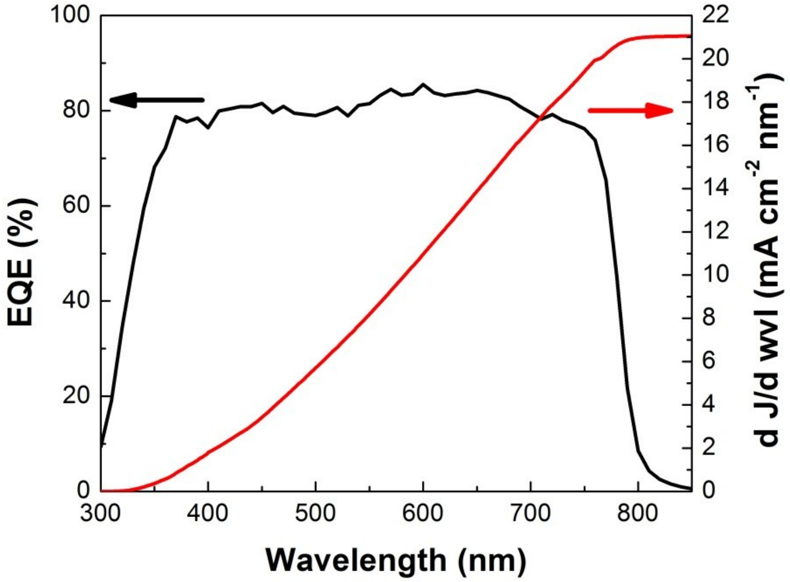

Figure S4. Typical EQE spectrum of type I devices.

Glass/ITO/TiO_2/ $CH_3NH_3PbI_3$/Spiro-OMeTAD/Au mini-modules (type II)

Glass substrates with ITO electrodes were purchased from Colorado Concept Coatings, and the P1 patterning (see Figure S5) was done in-house with a laser tool. The ITO-coated glass was then cleaned in ultrasonic baths of detergent, deionized water, acetone, and iso-propanol, each for 10 minutes, and next, it was transferred into an Angstrom Engineering evaporation system, equipped with an electron beam source. TiO_2 pellets purchased from Prof. Feierabend GmbH were evaporated at a rate of 1 Å/s onto ITO substrates, using a partial O_2 pressure of 1.7 x 10^{-4} Torr during the deposition, to maintain the stoichiometry of the film. To make the perovskite precursor solution, $Pb(CH_3CO_2)_2 \cdot 3H_2O$, $PbCl_2$, and CH_3NH_3I were dissolved in DMF. The concentration of the lead source, $Pb(CH_3CO_2)_2 \cdot 3H_2O$, together with $PbCl_2$, was 0.8 M, while the concentration of CH_3NH_3I was 2.4 M (Pb : CH_3NH_3I I = 1:3). The $PbCl_2$ molar fraction in the lead source was around 30%. The precursor solution was stirred at room temperature for 10 min, and then spin-coated at 3000 rpm for 60 s onto the TiO_2 layer. The obtained films were annealed on a hot plate at 130 °C for 10 min to form a perovskite crystal structure. After that, an 80 mg/ml spiro-OMeTAD solution, with 17.5 μl of lithium bis(trifluoromethanesulfonyl) imide (520 mg/ml in acetonitrile) and 28.5 μl of 4-tert-butylpyridine, was spin-casted onto the perovskite films. All of the spin-coating processes mentioned above were performed in a N_2-filled glove-box. The perovskite films coated with spiro-OMeTAD were then exposed to air overnight for spiro-OMeTAD oxygen doping. The P2 and P3 patterning (Figure S5) were performed within nitrogen atmosphere by using a knife mounted on a computer-controlled xyz-stage. The P2 patterning was carried out before the deposition of Au. The pressure was set in order to fully remove the TiO_2 layer ensuring a low contact resistance at the interconnect. Then, after Au deposition, the P3 patterning completed the device fabrication. The mini-modules consist of 4 cells with the area of 1 cm^2 each.

Initial *J-V* curves were measured in a nitrogen glove-box (kept at 25 ^oC) under simulated AM1.5G light using Abet Sun 2000 solar simulator (calibrated with an KG5 band pass equipped ISE Fraunhofer certified Si photodiode), in both forward and reverse directions with a scan rate of 4.9 V/s. The cells were then were tracked at the maximum power point (MPPT) for 180 s in order to get the stabilized value. Illumination mask was not used for *J-V* measurements. The average MPPT efficiency of the devices was around 10%. The EQE spectra were measured with a photospectrometer setup (Bentham PVE300) by illuminating the solar cell with a modulated monochromatic light (Xe and quartz halogen lamps). The spectral resolution is 5 nm. The typical *I-V* curve, EQE spectrum and the average performance of 14 identical devices are shown in Figures S6 and S7.

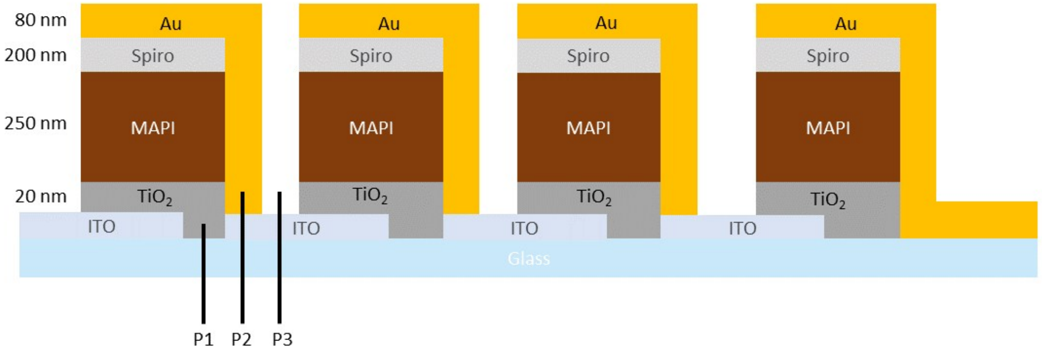

Figure S5. Schematic description of the type II mini-module device structure.

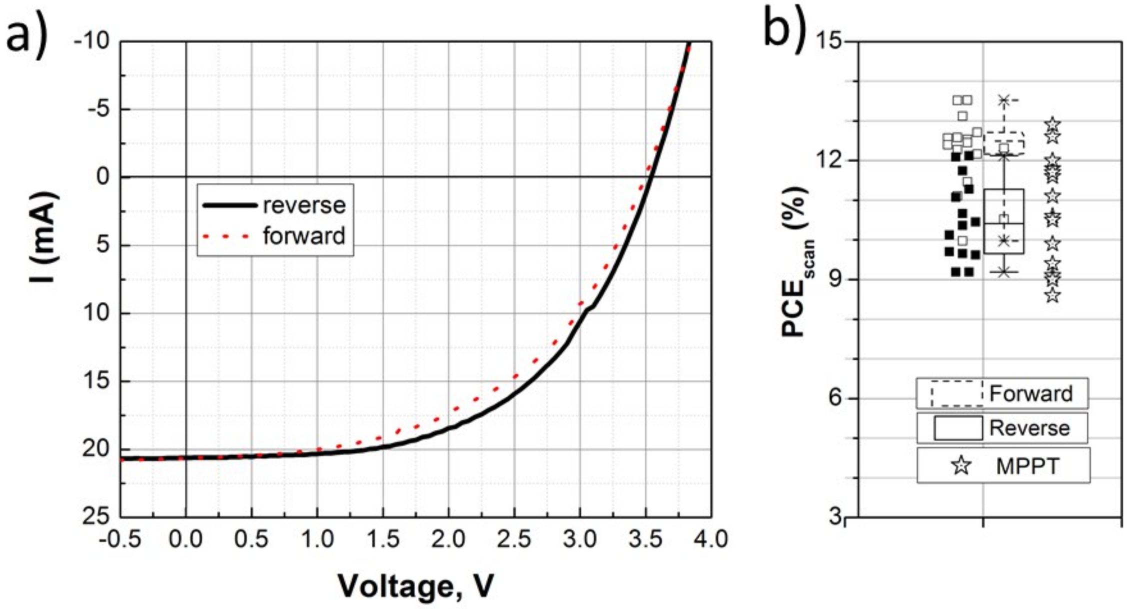

Figure S6. (a) Typical *I-V* characteristic of the mini-modules (type II devices), and (b) average performance of the manufactured devices.

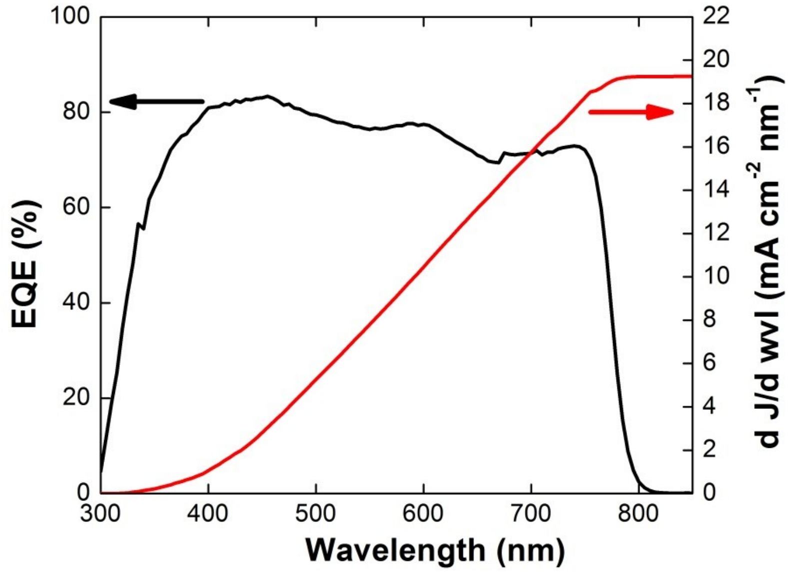

Figure S7. Typical EQE spectrum of the cell comprising the mini-modules (type II devices).

Degradation experiments

Outdoor degradation experiments were performed in Sede Boqer, Israel (Lat. 30.8°N, Lon. 34.8°E, Alt. 475 m) following the ISOS-O-1 protocol in March–May 2017. The devices were mounted on a fixed-angle (30°) platform at open circuit during daytime (from 10:00 to 17:00) and kept in the dark in a glove-box at night. Figure S8 shows the global sun radiation power (P_{in}) and ambient temperature during the outdoor experiment presented in the main text (Figures 2a and 3a). It should be noted that the sunlight spectrum measured at noontime ± 2–3 hours at Sede Boqer is very close to the AM1.5G spectrum.[2]

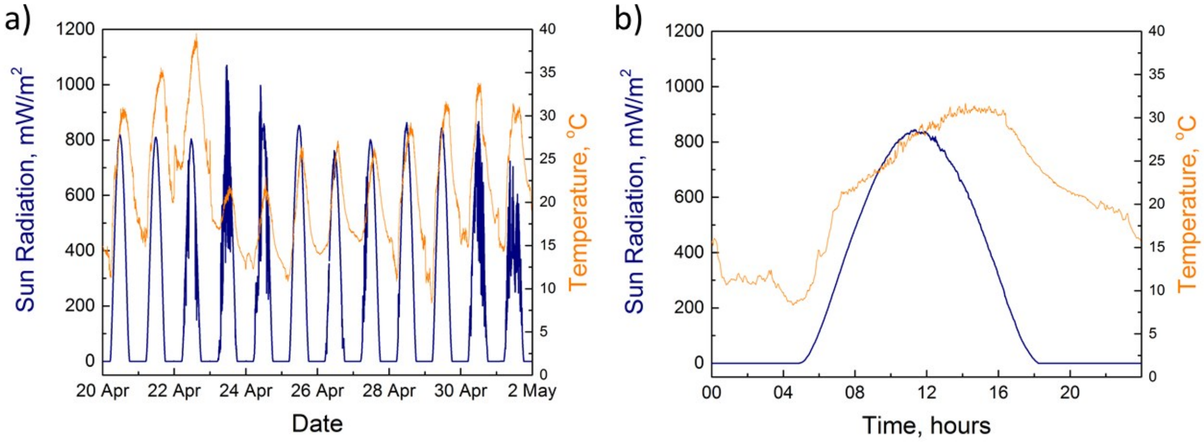

Figure S8. (a) Sun radiation hitting the cells on the fixed-angle platform and ambient temperatures in Sede Boqer during the outdoor experiment shown in Figures 2a and 2b. (b) The same during one day.

The *J-V* curves were measured three times a day with a Keithley 2401 source meter under the illumination of an AAA class Oriel VeraSol LSS-7120 solar simulator. The voltage sweeps for type I cells (type II mini-modules) were performed in the range -0.2 to 1.2 V (-0.5 to 4.0 V) in forward and reverse sweep directions with a scanning rate of 40 mV/s (125 mV/s). Illumination mask was not used for *J-V* measurements. Only the results for the reverse sweep are shown in the manuscript for clarity. Type II mini-modules were additionally preconditioned at open circuit for 5 minutes under illumination prior to each *J-V* measurement to avoid the impact of fast light-soaking effect.

Indoor degradation experiments - Long-term stability testing under continuous light illumination (AM 1.5G, 1 kW/m^2) was performed according to ISOS-L-1 protocol standards using a setup consisting of an ISOSun wide-area solar simulator with a metal halide lamp (metal halide display/optic lamp HMI from Osram calibrated with Reference Cell and Meter, 91150V, Newport) in ambient air. The ambient conditions were monitored by temperature (60 °C) and intensity sensors, and recorded periodically along with the solar cell parameters. The solar cell parameters were traced in situ via periodic *J-V* (forward sweep direction with a scanning rate of 333 mV/s) measurements every 10 minutes. Illumination mask was not used for *J-V* measurements. Between the measurements the cells were kept at open circuit condition.

References

1. P. Van de Weijer,P.C.P. Bouten, S. Unnikrishnan, H.B. Akkerman, J. J. Michels, T. M. B. van Mol, High-Performance Thin-Film Encapsulation for Organic Light-Emitting Diodes. *Org. Electron.* 44, 94–98 (2017).
2. L. N. Inasaridze, A. I. Shames, I. V. Martynov, B. Li, A. V. Mumyatov, D. K. Susarova, E. A. Katz, P. A. Troshin, Light-induced generation of free radicals by fullerene derivatives: an important degradation pathway in organic photovoltaics? *J. Mater. Chem. A* 5, 8044-8050 (2017).